Half-Skyrmions and the equation of state for compact-star matter

Huan Dong,[1] T. T. S. Kuo,[1] Hyun Kyu Lee,[2] R. Machleidt,[3] and Mannque Rho[4]

[1]*Department of Physics and Astronomy, Stony Brook University, Stony Brook, New York 11794, USA*
[2]*Department of Physics, Hanyang University, Seoul 133-791, Korea*
[3]*Department of Physics, University of Idaho, Moscow, Idaho 83843, USA*
[4]*Institut de Physique Théorique, CEA Saclay, 91191 Gif-sur-Yvette cédex, France and Department of Physics,
Hanyang University, Seoul 133-791, Korea*

The half-skyrmions that appear in dense baryonic matter when skyrmions are put on crystals modify drastically hadron properties in dense medium and affect strongly the nuclear tensor forces, thereby influencing the equation of state (EoS) of dense nuclear and asymmetric nuclear matter. The matter comprising half-skyrmions has vanishing quark condensate but nonvanishing pion decay constant and could be interpreted as a hadronic dual of strong-coupled quark matter. We infer from this observation combined with certain predictions of hidden local symmetry in low-energy hadronic interactions a set of new scaling laws—called "new-BR"—for the parameters in nuclear effective field theory controlled by renormalization-group flow. They are subjected to the EoS of symmetric and asymmetric nuclear matter, and are then applied to nuclear symmetry energies and properties of compact stars. The changeover from the skyrmion matter to a half-skyrmion matter that takes place after the crossover density $n_{1/2}$ provides a simple and natural field theoretic explanation for the change of the EoS from soft to stiff at a density above that of nuclear matter required for compact stars as massive as $\sim 2.4 M_\odot$. Crossover density in the range $1.5 n_0 \lesssim n_{1/2} \lesssim 2.0 n_0$ was employed, and the possible skyrmion half-skyrmion coexistence or crossover near $n_{1/2}$ is discussed. The novel structure of the tensor forces and the EoS obtained with the new-BR scaling is relevant for neutron-rich nuclei and compact-star matter and could be studied in RIB (rare isotope beam) machines.

I. INTRODUCTION

The topological soliton called skyrmion [1] has turned out to be exceedingly pervasive in a variety of space-time dimensions ranging from 3 to 5 in many areas of physics [2] and was beautifully observed in such systems as quantum Hall or cold atoms and more recently in a monoatomic magnetic film (see, e.g., [3]). In contrast, the situation with its role in nuclear physics was much less clear and with somewhat limited success. In this note, we make an attempt to uncover the power, hitherto unexploited, of skyrmion in strong interaction physics focusing on nuclear and dense matter. In contrast to condensed matter, the effect of skyrmion structure in strong interactions turns out to be indirect and hence much less transparent. In this work we show with simple plausible arguments that the skyrmion picture can indeed make a novel prediction on the properties of compact stars that has not been made thus far by other approaches.

The arguments made in formulating the theoretical framework are neither rigorous nor completely unambiguous. Although the crystal structure which is valid in the large N_c limit could be applicable at very large density, it is not clear that it can be used in the density regime that we are concerned with, which will be a few times the normal nuclear matter density. What we will be exploiting is, however, the topological structure provided by the skyrmion configuration, which is insensitive to spatial symmetry. In proceeding we will rely on what nature indicates at normal densities and then extrapolate to high densities using a hidden local symmetry (HLS) structure with well-defined degrees of freedom.

The starting point of our work is that when a large number of skyrmions as baryons are put on a face-centered-cubic (FCC) crystal to simulate dense matter, the skyrmion matter undergoes a transition to a matter consisting of half-skyrmions [4] in CC configuration at a density that we shall denote as $n_{1/2}$. This density is difficult to pin down precisely but it is more or less independent of the mass of the dilaton scalar, the only low-energy degree of freedom that is not well known in free space. It was estimated to lie typically at between 1.3 and 2 times the normal nuclear matter density n_0 [5].

The half-skyrmion phase, made up of fractionized baryon numbers, is characterized by the quark condensate $\langle \bar{q} q \rangle$ that vanishes on the average in the unit cell with, however, chiral symmetry still broken, so the pion is present. It likely has an inhomogeneous spatial distribution of baryon density. There is no obvious order parameter for the "transition" although there can be higher-dimension field operators representing an emergent symmetry that could be identified at quantum level. What can distinguish the two "phases" are the different degrees of freedom with different topological charges.

Among the predictions made so far with the half-skyrmion phase, the most striking one—which is the main object of this article and has not been made by other approaches—was that the presence of $n_{1/2}$ strongly modifies the tensor forces in nuclear interactions and in particular the symmetry energy at densities $n > n_{1/2}$ [6,7].

In this note, we confront our predictions with nature by translating the (semi)classical results of [6] into the parameters of an effective Lagrangian having chiral symmetry and conformal symmetry, and then do a quantum–effective-field-theory

(EFT) calculation for nuclear matter and compact-star matter using a renormalization-group (RG)-based formalism [8]. For the range $n_{1/2} = (1.5\text{–}2.0)\,n_0$ considered in [6], we have applied our formalism to neutron star calculations and a comparison of our results with the recently discovered two-solar-mass neutron star [9] will be discussed. An interesting result of the calculation is that the skyrmion-half-skyrmion crossover makes the EoS stiffer at the crossover density $n_{1/2}$ and beyond, thereby leading to more massive stars.

In a nutshell, our strategy is as follows. Up to the nuclear matter density n_0, our nuclear effective field theory will be guided by symmetries of low-energy QCD (such as chiral symmetry, hidden local symmetry, etc.) backed by nuclear phenomenology available up to density near n_0. There the effective Lagrangian will be endowed with parameters suitably scaling in the vacuum sliding with the density. We will assume that one can use the same EFT up to the density $n_{1/2}$ at which half-skyrmions appear which we take to be above but not far above n_0. Above $n_{1/2}$ for which there are neither experimental data nor model-independent theoretical tools available, we will take the properties indicated by the skyrmion-half-skyrmion transition based on hidden local symmetric Lagrangian and certain predicted property of hidden local fields as the chiral critical point is approached. The effective Lagrangian so given is then translated into an effective nuclear field theory that is subject to many-body techniques that account for high order quantum effects.

II. NEW-BR IN THE HALF-SKYRMION PHASE

What plays a key role in our development is the nuclear symmetry energy computed in [6] in dense skyrmion matter. There it was found that the symmetry energy E_{sym} figuring in the energy per particle of asymmetric nuclear matter at density n in the form,

$$E(n, \alpha) = E(n, \alpha = 0) + E_{\text{sym}}(n)\alpha^2 + \mathcal{O}(\alpha^4), \quad (2.1)$$

where $\alpha = (n_n - n_p)/(n_n + n_p)$ with $n_n(n_p)$ the number density of neutrons (protons) is given by

$$E_{\text{sym}} \approx \frac{1}{8\lambda_I}, \quad (2.2)$$

where λ_I is the isospin moment of inertia obtained by rotational quantization of the multi-skyrmion system which is given by an integral over the unit cell of a certain combination of the skyrmion configuration. We should understand that this is a quasiclassical potential energy contribution coming at $\mathcal{O}(1/N_c)$ in the large N_c expansion and contains no kinetic energy term. In what follows, we shall take into account quantum corrections arising from nuclear correlations that are higher order in $1/N_c$. For the moment we focus on (2.2). A striking feature of (2.2) discovered in [6] is a cusp at $n_{1/2}$ of the symmetry energy which decreases from n_0 to $n_{1/2}$ and then increases for $n > n_{1/2}$. Now given the classical nature of (2.2) and the neglect of the kinetic energy term, one cannot expect this feature to appear unscathed in experiments. To confront nature, one has to go beyond the classical approximation of the skyrmion crystal. How to systematically make quantum corrections within the skyrmion crystal approach is not yet

known. What we shall instead do is "translate" the classical result of [6] into the framework of an effective field theory treated at mean field of a HLS Lagrangian [10] that contains all relevant degrees of freedom at the energy scale involved, i.e., baryons, pions, and vector mesons. There is of course a certain arbitrariness in doing this but we shall rely on what nature indicates. In addition, a dilaton scalar denoted χ is introduced to account for the spontaneously broken conformal symmetry as precisely defined in [11]. The work in [6] uses the nonlinear sigma model, involving only pions and baryons (emerging as skyrmions). However the nonlinear sigma model Lagrangian is gauge equivalent to the HLS Lagrangian, hence can capture the physics of vector mesons as was proposed in [12]. Our strategy which is consistent with the spirit of the renormalization group is then to do effective field theory calculation with this Lagrangian, with the parameters of which "running" with the *intrinsic* medium dependence as formulated in [12]. We will refer to this medium dependence as "BR scaling."

We will now describe how the cusp structure in (2.2) can be reproduced by an effective Lagrangian in mean field.

Up to the density $n_{1/2}$, our effective Lagrangian will carry the parameters scaling as introduced in [12]. Let us call it "old-BR." They are of the form,

$$m_V^*/m_V \approx m_N^*/m_N \approx f_\pi^*/f_\pi \equiv \Phi_I, \quad (2.3)$$

and

$$g_V^*/g_V \approx 1, \quad (2.4)$$

where the asterisk represents density dependence, f_π is the pion decay constant, the subscripts N and V stand, respectively, for the nucleon and the vector mesons $V = \rho, \omega$,[1] and g_V is the hidden gauge coupling constant g standing for both $V = \rho, \omega$ [13]. It was assumed [12,13] that the flavor $U(2)$ symmetry applies to (ρ, ω) in baryonic matter up to the normal nuclear matter density n_0 and will be assumed in what follows, up to $n_{1/2}$ as it does in matter-free space. However, at $n \gtrsim n_{1/2}$, the fractionization of the skyrmions produces a change in the intrinsic scaling as [6]

$$m_\rho^*/m_\rho \equiv \Phi_{II}^\rho, \quad m_N^*/m_N \equiv \Phi_{II}^N = y(n), \quad (2.5)$$

where $y(n)$ is an order 1 constant that is more or less density independent as explained below. The scaling Φ_{II}^ρ is unknown except (perhaps) very near chiral transition. It needs not scale in the same way as Φ_I does as explained below. Very near chiral transition at $n = n_c$, however, the HLS theory has, whether viable or not, a definite prediction thanks to the "vector manifestation fixed point (VM)" at which the matching of both the vector and axial-vector correlators gives [10]

$$m_\rho^*/m_\rho \approx g_\rho^*/g_\rho \to \langle \bar{q}q \rangle^*/\langle \bar{q}q \rangle, \quad n \to n_c, \quad (2.6)$$

where q stands for chiral quark field. Unless we assume that $U(2)$ symmetry holds in medium—which we will not as explained below—the hidden local symmetry argument does not give any prediction as to how the ω mass and the ω-NN

---

[1]Whenever necessary, as will be the case for $n > n_{1/2}$, we will specify whether it is ρ or ω.

coupling behave in medium for $n > n_{1/2}$. For simplicity, we will simply take

$$m_\omega^*/m_\omega \approx m_\rho^*/m_\rho. \qquad (2.7)$$

As for the ω-NN coupling $\equiv g_\omega$, it is very much subtler and we will specify it later. We will call (2.5)–(2.7) "new BR." The difference from the old BR is lodged in the density regime $n \gtrsim n_{1/2}$.

There are two points to note here:

(i) One is that at $n_{1/2}$ the scaling parameter changes from the pion decay constant scaling as $(f_\pi^*/f_\pi)^2 \sim \langle \bar{q}q \rangle^*/\langle \bar{q}q \rangle$ to the hidden local symmetry coupling constant g_ρ scaling linearly as in (2.6). This changeover was already observed in [13] from phenomenology. Because g_ρ is directly connected, via renormalization group flow, to the quark condensate which is the *bona fide* order parameter of chiral symmetry in the chiral limit, near the VM fixed point, it is the vector meson mass $\propto g_\rho$ that carries information on chiral symmetry, not the pion decay constant. This changeover of the scaling from f_π^* to g_ρ^* that accounts for that Φ_I and Φ_{II} need not have the same behavior in density is reflected in the half-skyrmion phase in that the pion decay constant drops only slowly in contrast to the quark condensate which drops to zero at $n_{1/2}$. It is important to note that the hidden gauge coupling g_ρ scales in the same way as the ρ-meson mass does at high density whereas at low density up to $n_{1/2}$, the gauge coupling stays unscaling. This difference will turn out to have a drastic effect on the ρ tensor force for $n > n_{1/2}$.

(ii) The second point, also connected to the slowly dropping pion decay constant, is that the nucleon mass scales little beyond $n_{1/2}$, remaining nonzero at the chiral transition. This resembles—and we believe is related to—the nucleon mass in the parity-doublet nucleon model where there is a somewhat large chirally invariant mass m_0 that remains at the transition [14]. In our application to be given below, we will consider $m_0 \sim (0.7$–$0.8)m_N$.

That the new BR affects the nuclear tensor forces across the density $n_{1/2}$ was explained in [6,7]. So we will skip the details and briefly summarize only the main features that we will need below.

If one takes the nucleon to be heavy while other hadrons, i.e., mesons, are light, then one can take the nonrelativistic approximation for the nucleons and write the effective tensor forces in medium in the usual form with the parameters of the Lagrangian carrying the intrinsic density dependence à la BR scaling. The two tensor forces contributed by the pion exchange and the ρ exchange are given in the standard form with the masses and coupling constants replaced by the starred quantities. Dividing by the vacuum quantity $(C_M)^2 = (\frac{f_{MN}}{4\pi})^2$ and writing $x_M^* = m_M^* r$, we have the in-medium π and ρ tensor forces in the form,

$$V_M^T(r)/(C_M)^2 = S_M \tau_1 \cdot \tau_2 S_{12}(R_M^*)^2 m_M^\star Y(x_M^*), \qquad (2.8)$$

with

$$Y(x_M^*) = \left[\frac{1}{(x_M^*)^3} + \frac{1}{(x_M^*)^2} + \frac{1}{3x_M^*} \right] e^{-x_M^*}, \qquad (2.9)$$

where $M = \pi, \rho$, $S_{\rho(\pi)} = +1(-1)$, and $R_M^* = f_{MN}^*/f_{MN}$. The crucial (very well-known) feature to note is that the two forces come with an opposite sign.

As argued in [6], the pion tensor force can be taken unscaling in all relevant density range. In fact, one can verify explicitly that using suitably scaling parameters for all parameters that enter in the pion tensor force, such as f_π, etc., gives results that are close to those obtained by taking *all* the parameters unscaled [7]. Thus $R_\pi^* \approx 1$ and $m_\pi^* \approx m_\pi$ in Eq. (2.8). As for the ρ tensor, what remains to be determined is the scaling of R_ρ^*. It follows straightforwardly from (2.3) and (2.5) that

$$R_\rho^* = \frac{g_V^* m_V^* m_N}{g_V m_V m_N^*} \approx \frac{g_V^*}{g_V} \approx 1 \ \text{ for } \ 0 \lesssim n \lesssim n_{1/2}, \qquad (2.10)$$

and

$$R_\rho^* = \frac{g_\rho^* m_\rho^* m_N}{g_\rho m_\rho m_N^*} \approx \frac{g_\rho^*}{g_\rho} \Phi_{II}^\rho \big/ y(n)$$
$$\approx \left(\Phi_{II}^\rho \right)^2 \big/ y(n) \ \text{ for } \ n_{1/2} < n \lesssim n_c, \qquad (2.11)$$

where n_c is the putative chiral transition density. Because $g_\rho^*/g_\rho \sim \Phi_{II}^\rho$ in Region II, we have (2.11) with R_ρ^* scaling as $\sim (\Phi_{II}^\rho)^2$ for $n \gtrsim n_{1/2}$ and this makes a big change in the behavior of the net tensor force. Up to density $n \approx n_0$, the scaling Φ_I makes the total tensor strength weakened at increasing density because the increased ρ tensor eats into the pion tensor [7,15]. Recently this mechanism was shown to explain the long-standing problem of the carbon 14 dating [16] which in turn determines how Φ_I scales up to n_0.[2] If the scaling Φ_I continued beyond n_0, then it would make the net tensor attraction vanish at $n \sim 2n_0$ [7]. Now with the new scaling, this behavior no longer holds. The simple prediction is that the net tensor-force strength will cease to drop at $n_{1/2}$. Just to have an idea of what this does, take $\Phi_{II} \approx \Phi_I$. A simple estimation shows that when density reaches $n \sim (2-3)n_0$, the ρ tensor becomes totally negligible. What remains is only the pion tensor. When this happens, π^0's could condense in a crystalline form as suggested in [6,7].

We now argue that an effective field theory at mean field with the tensor force that follows from the new BR can reproduce the cusp structure in the symmetry energy (2.2) seen in the skyrmion-crystal calculation. This can be seen from the fact that the symmetry energy is dominated by the tensor force [17,18]. A simple formula that captures the essential physics of the tensor forces is that of Brown and Machleidt [17] that we rewrite including the new BR,

$$E_{\text{sym}} \approx \frac{C}{\bar{E}} \langle V_T^2 \rangle, \qquad (2.12)$$

---

[2]It was suggested that this could also be explained by certain short-range three-body forces [19]. This of course does not mean that three-body forces are an *alternative* to the scaling mechanism. More on this point in Discussions section.

where C is a known constant, $\bar{E}$ is the average energy appropriate for the tensor force, ≈ 200 MeV, and V_T is the radial part of the tensor force that includes the effect of the new BR. There is again the kinetic term which we will ignore as before. In the form of (2.12), the cusp structure then follows immediately from the discussions given above for the behavior of the tensor forces across $n_{1/2}$, i.e., the decrease of the net tensor force strength from n_0 to $n_{1/2}$ and its increase after $n_{1/2}$ with the pion tensor taking over the strength. We take this as a support for the skyrmion crystal—mean-field EFT transcription.

We will see below how nuclear correlations that go beyond the mean-field approximation modify this cusp structure. It actually smoothes it without completely eliminating it. The effective field theory anchored on the Lagrangian endowed with the new BR is applied first to nuclear matter and then to compact-star matter addressing the issue of the maximum neutron-star mass versus radius.

III. NUCLEAR EQUATION OF STATE

So far we have been discussing qualitative features impacted by the new BR. We now confront quantitatively the scaling relations (2.3), (2.5), (2.10), and (2.11) with the properties of symmetric as well as asymmetric nuclear matter. We incorporate the new BR in the nuclear effective field theory in which the RG-implemented $V_{\text{low}-k}$ plays a key role. More specifically, we apply the new-BR scalings discussed in Sec. II to nuclear matter, both symmetric and asymmetric, and to the nuclear symmetry energy. The special features in the new BR are the scaling of the nucleon mass $y(n)$ and that of the vector coupling g. As we shall elaborate in the discussion section, these features are thought to be closely connected to how (most of) the nucleon mass is generated in the strong interactions.

Before continuing, let us concisely recapitulate how the new BR enters into an RG-implemented EFT. As argued in [13], it involves two decimations in the RG sense. Starting with an effective chiral Lagrangian, one first decimates in matter-free space from the chiral scale $\Lambda_\chi \sim 4\pi f_\pi \sim 1$ GeV down to the first decimation scale $\Lambda \sim 3$ fm^{-1}. What results is the $V_{\text{low}-k}$ that is used in our calculation. Then doing many-body calculations for nuclear systems with the parameters of $V_{\text{low}-k}$ running à la new BR amounts to doing the second decimation. In fact this second decimation is equivalent to doing a Landau Fermi-liquid theory calculation as formulated in [13]. In doing this, we are ignoring three-body and higher-body forces. One should, however, recognize that part of many-body force effects are embedded in the new BR. One can think of this as a sort of duality between the two as will be elaborated later.

To suitably take into account the features mentioned above into a high-order effective field theory calculation, we shall carry out our calculations using the realistic BonnS potential [20]; this potential is an extension of the one-boson-exchange BonnA potential [21] with the provision that the nucleon and meson mass as well as the vector coupling be scaled à la new BR. As discussed in Sec. II, we employ the following two-region scalings characterized by the transition densities $n_{1/2}$ and n_c (respectively, for the skyrmion-half-skyrmion and

chiral transitions). For density $0 < n < n_{1/2}$ (Region I), we use[3]

$$\frac{m_M^*}{m_M} = \frac{m_N^*}{m_N} = \Phi_I(n); \quad \Phi_I(n) = \frac{1}{1 + c_I \frac{n}{n_0}}, \quad (3.1)$$

and

$$R_\rho^* = 1. \quad (3.2)$$

In the above $M = (V, S)$ and N stand, respectively, for meson (both vector and scalar) and nucleon. For density $n_{1/2} < n < n_c$ (Region II), we use

$$\frac{m_M^*}{m_M} = \Phi_{II}^M(n); \quad \Phi_{II}^M(n) = \frac{1}{1 + c_{II} \frac{n}{n_0}} \quad (3.3)$$

for mesons and

$$\frac{m_N^*}{m_N} = \Phi_{II}^N(n) = y(n) \quad (3.4)$$

for nucleons. We use the R^* scaling in II as

$$R_\rho^* = \frac{g_\rho^*}{g_\rho} \Phi_{II}^M(n)/y(n) = \left(\Phi_{II}^M\right)^2 / y(n). \quad (3.5)$$

The above scaling functions Φ_I and Φ_{II} are in general not continuous at the boundary density $n_{1/2}$. This discontinuity may be a mere artifact of the simplification we are adopting. In the present work, as to be discussed later, we shall choose the parameters contained in them so that these two functions are nearly continuous (to avoid drastic discontinuity) at $n_{1/2}$. In addition, we shall employ two Fermi-Dirac functions to smoothly join the scaling functions Φ_I and Φ_{II} so that the resulting scaling function Φ is ensured to be continuous at the boundary. A similar procedure will also be employed for the R^* scalings in the two regions. To illustrate, the smoothed scaling function Φ is constructed as

$$\Phi = F_<(n_{1/2})\Phi_I + F_>(n_{1/2})\Phi_{II}, \quad (3.6)$$

with

$$\begin{aligned} F_<(n_{1/2}) &= [1 + e^{(n-n_{1/2})/\delta}]^{-1}, \\ F_>(n_{1/2}) &= [1 + e^{(n_{1/2}-n)/\delta}]^{-1}, \end{aligned} \quad (3.7)$$

where δ is a smoothness parameter. In the present work, we shall use $\delta/n_0 \simeq 0.05$–0.10. It turns out that within this range our results are satisfactorily stable with respect to δ.

We have adopted the following procedure for choosing the parameters of the above scaling functions. First we require the parameters in Region I so that they satisfactorily reproduce the empirical nuclear matter saturation properties (saturation density $n_0 \simeq 0.16$ fm^{-3} and average energy per nucleon $E_0/A \simeq -16$ MeV at saturation). The choice for the parameters in Region II will be addressed later. We shall calculate

---

[3]We must stress that except for low density $\lesssim n_0$ (and possibly high density near the chiral transition point in the chiral limit as predicted in HLS), the precise form of the scaling is not known, so what we take should be understood as more of a convenient parametrization guided, whenever feasible, by phenomenology. Furthermore there is nothing that suggests that the scaling should be identical for all mesons.
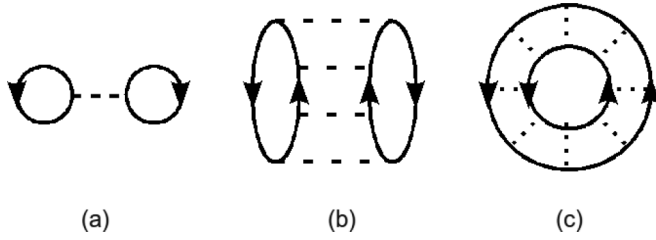
FIG. 1. Diagrams included in the all-order *pphh* ring-diagram summation for the ground-state energy of nuclear matter. Each dashed line represents a $V_{\text{low}-k}$ vertex.

n_0 and E_0/A using a low-momentum ring-diagram approach [8,22–25], where the *pphh* ring diagrams are summed to all orders within a model space of decimation scale Λ. Few low-order (first, fourth, and eighth order) such diagrams are displayed in Fig. 1. Note that each vertex of the diagrams is a low-momentum interaction $V_{\text{low}-k}$ which is obtained from a realistic *NN* potential V_{NN} using a renormalization group approach where the momentum components beyond a decimation scale Λ are integrated out [26–29].

More precisely $V_{\text{low}-k}$ is given by the following T-matrix equivalence equations:

$$T(k', k, k^2) = V_{NN}(k', k)$$
$$+ \frac{2}{\pi} \mathcal{P} \int_0^\infty \frac{V_{NN}(k', q)T(q, k, k^2)}{k^2 - q^2} q^2 dq, \tag{3.8}$$

$$T_{\text{low}-k}(k', k, k^2) = V_{\text{low}-k}(k', k) + \frac{2}{\pi} \mathcal{P} \int_0^\Lambda$$
$$\times \frac{V_{\text{low}-k}(k', q)T_{\text{low}-k}(q, k, k^2)}{k^2 - q^2} q^2 dq, \tag{3.9}$$

$$T(k', k, k^2) = T_{\text{low}-k}(k', k, k^2); \quad (k', k) \leqslant \Lambda. \tag{3.10}$$

In the present work the above V_{NN} is chosen to be the realistic BonnS [20] *NN* interaction. (The new-BR scalings we have established above enter into the meson parameters as well as the nucleon mass of this potential with the varying density.) $\mathcal{P}$ denotes principal-value integration and the intermediate state momentum q is integrated from 0 to ∞ for the whole-space T and from 0 to Λ for $T_{\text{low}-k}$. Because we shall calculate the nuclear symmetry energy $E_{\text{sym}}(n)$ up to $n \sim 5n_0$, we shall use $\Lambda = 3$ fm^{-1} [8]. The above $V_{\text{low}-k}$ preserves the low-energy phase shifts in the vacuum (up to energy Λ^2) and the deuteron binding energy of V_{NN}. (For example, the deuteron binding energy given by $V_{\text{low}-k}$ of $\Lambda = 2.0$ and 3.0 fm^{-1} are both -2.226 MeV.) Because $V_{\text{low}-k}$ is obtained by integrating out the high-momentum components of V_{NN}, it is a smooth "tamed" potential which is suitable for being used directly in many-body calculations. The familiar HF approximation for nuclear matter corresponds to the inclusion of only the first-order diagram (a) of the figure. In contrast, the *pphh* ring diagrams such as those shown in Fig. 1 are included to all orders in our nuclear matter calculations.

With such ring diagrams summed to all orders [22,23], the ground-state energy of asymmetric nuclear matter is expressed

as $E(n, \alpha) = E^{\text{free}}(n, \alpha) + \Delta E(n, \alpha)$ where E^{free} denotes the energy for the noninteracting system and ΔE, the energy shift due to the *NN* interaction, is given by the all-order sum of the *pphh* ring diagrams as illustrated in Fig. 1. We include in general three types of ring diagrams, the proton-proton, neutron-neutron, and proton-neutron ones. The proton and neutron Fermi momenta are, respectively, $k_{Fp} = (3\pi^2 n_p)^{1/3}$ and $k_{Fn} = (3\pi^2 n_n)^{1/3}$, where n_p and n_n denote, respectively, the proton and neutron density. The asymmetric parameter is $\alpha \equiv (n_n - n_p)/(n_n + n_p)$. With such ring diagrams summed to all orders, we have

$$\Delta E(n, \alpha) = \int_0^1 d\lambda \sum_m \sum_{ijkl<\Lambda} Y_m(ij, \lambda)$$
$$\times Y_m^*(kl, \lambda)\langle ij|V_{\text{low}-k}|kl\rangle, \tag{3.11}$$

where the transition amplitudes Y are obtained from a *pphh* RPA equation [22,23]. Note that λ is a strength parameter, integrated from 0 to 1. The above ring-diagram method reduces to the usual HF method if only the first-order ring diagram is included. In this case, the above energy shift becomes $\Delta E(n, \alpha)_{HF} = \frac{1}{2} \sum n_i n_j \langle ij|V_{\text{low}-k}|ij\rangle$ where $n_k = (1, 0)$ if $k(\leqslant, >)k_{Fp}$ for proton and $n_k = (1, 0)$ if $k(\leqslant, >)k_{Fn}$ for neutron.

The above $V_{\text{low}-k}$ ring-diagram framework was applied to symmetric and asymmetric nuclear matter [22,23] and to the nuclear symmetry energy [8]. This framework has also been tested by applying it to dilute cold neutron matter in the limit that the $^1S_0$ scattering length of the underlying interaction approaches infinity [24,25]. This limit—which is a conformal fixed point—is usually referred to as the unitary limit, and the corresponding potentials the unitarity potentials. For many-body systems at this limit, the ratio $\xi \equiv E_0/E_0^{\text{free}}$ is expected to be a universal constant of value ~ 0.44. (E_0 and E_0^{free} are, respectively, the interacting and noninteracting ground-state energies of the many-body system.) The above ring-diagram method was used to calculate neutron matter using several very different unitarity potentials (a unitarity CDBonn potential obtained by tuning its meson parameters, and several square-well unitarity potentials) [24,25]. The ξ ratios given by our calculations for all these different unitarity potentials are all close to 0.44, in good agreement with the quantum Monte Carlo results (see [25], and references quoted therein). In fact our ring-diagram results for ξ are significantly better than those given by HF and BHF (Brueckner HF) [24,25]. It is desirable that the above unitary calculations have provided satisfactory results, supporting the reliability of our $V_{\text{low}-k}$ ring-diagram framework for calculating the nuclear matter EoSs.

IV. RESULTS

We recall that the new BR has an assumption which is not an immediate consequence of chiral symmetry. Specifically the premise of the vector manifestation associated with hidden local symmetry states that as one approaches the VM fixed point, $m_\rho^*/m_\rho \to g_\rho^*/g_\rho \to 0$, which is not dictated by chiral symmetry alone. Here we will take the point of view that the vector manifestation property is operative after the half-skyrmion onset density $n_{1/2}$.
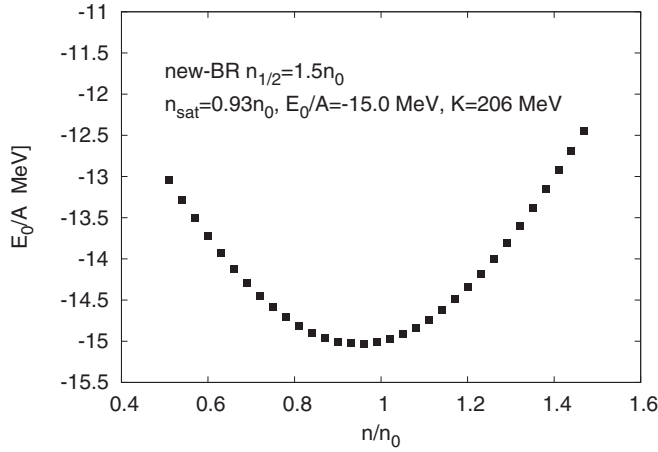
FIG. 2. New-BR EoS for symmetric nuclear matter calculated with $n_{1/2} = 1.5n_0$. See text for more explanations.

Let us first consider the EoS of symmetric nuclear matter in the low density region ($n \lesssim n_{1/2}$), the main purpose here being the choice of the c_I parameters so that the empirical saturation properties of symmetric nuclear matter are satisfactorily reproduced. In Fig. 2, we present our results for symmetric nuclear matter calculated with parameters $c_I = 0.130$ for nucleon and ρ meson, $=0.121$ for σ meson, and $= 0.139$ for ω meson.[4] The EoS of this figure gives ground-state energy per nucleon $E_0/A = -15$ MeV, saturation density $n_{sat} = 0.93n_0$, and compression modulus $K = 208$ MeV, all in satisfactory agreement with the empirical values. [Here and in Fig. 2 E_0/A is the same as $(E(n, \alpha = 0) - m_N)$ of Eq. (2.1)]. The above calculation has employed $n_{1/2} = 1.5n_0$. As to be presented later, we have also carried out calculations with $n_{1/2} = 2n_0$ and the saturation properties given by them are nearly the same as the $n_{1/2} = 1.5n_0$ case. Recall that a decimation scale of $\Lambda = 3$ fm^{-1} was employed in the above calculation, and it will be used in what follows.

As discussed in [22,23], the use of realistic V_{NN} with the old BR [12,30,31] leads to satisfactory nuclear matter saturation properties. As seen in Fig. 2, the new BR does also lead to satisfactory nuclear matter saturation properties, even though these two scalings are different for $n \gtrsim n_{1/2}$. The main differences between them are in the scaling of the nucleon mass and the HLS coupling g. While the nucleon mass does scale in Region I with the change in $\langle \bar{q}q \rangle^*$, its scaling more or less stops at $y(n_{1/2})$ for $n > n_{1/2}$ and is assumed to change drastically only at n_c. The gauge coupling g on the other hand remains unchanged up to $n_{1/2}$ and drops roughly proportional to $\langle \bar{q}q \rangle^*$ afterwards as suggested in [13].

Before proceeding to the EoS for $n \gtrsim n_{1/2}$, let us first discuss the scaling parameters we have employed. The scaling functions we have used in Region I [(3.1) and (3.2)] are similar to those employed in the old BR [12,31] and Ericson (ER) [32] scalings. The ER scaling is based on the quark condensate

relation [32],

$$\frac{\langle \bar{q}q \rangle^*}{\langle \bar{q}q \rangle} = \frac{1}{1 + \frac{n \Sigma_{\pi N}}{f_\pi^2 m_\pi^2}}, \quad (4.1)$$

where $\Sigma_{\pi N} = 45 \pm 7$ MeV [33]. Then the ER scaling for hadrons in medium reads

$$\frac{m^*}{m} = \left(\frac{1}{1 + D\frac{n}{n_0}} \right)^{1/3}, \quad (4.2)$$

with $D = \frac{n_0 \Sigma_{\pi N}}{f_\pi^2 m_\pi^2}$. Using the empirical values for $(\Sigma_{\pi N}, n_0, f_\pi, m_\pi)$, we have $D = 0.35 \pm 0.06$. Note that for the low-density region this relation agrees well with the parametrization for the old BR [12,31],

$$\frac{m^*}{m} = 1 - C\frac{n}{n_0}, \quad (4.3)$$

where C is a constant of value ~ 0.15.

It may be noted that our new BR in Region I [(3.1) and (3.2)] is consistent with the above Ericson scaling in the $n < n_{1/2}$ region if the c_I scaling parameters are chosen to have values near $D/3 \simeq 0.12 \pm 0.02$. It is encouraging that the c_I parameters we have employed so as to give satisfactory nuclear matter saturation properties (Fig. 2) are indeed quite close to the value of $D/3$ given by QCD theories.

We now consider the EoS for $n > n_{1/2}$. In Fig. 3 we present results for two choices for the half-skyrmion onset densities, namely $n_{1/2} = 2.0$ and $1.5n_0$. In addition we also present the EoS [labeled (C) in the figure] obtained with the unscaled BonnS [20] potential. As seen this EoS does not have satisfactory nuclear matter saturation properties; it would give saturation density much higher than the empirical value of ~ 0.16 fm^{-3} as well as a saturation energy much lower than the empirical value of ~ -16 MeV. In contrast, the new-BR EoSs (A) and (B), respectively, for $n_{1/2} = 2.0$ and $1.5n_0$, both have satisfactory saturation properties. In calculating (A) and (B), we have used the same c_I parameters as listed earlier. Thus (A) and (B) are equivalent for $n < 1.5n_0$, both having the same
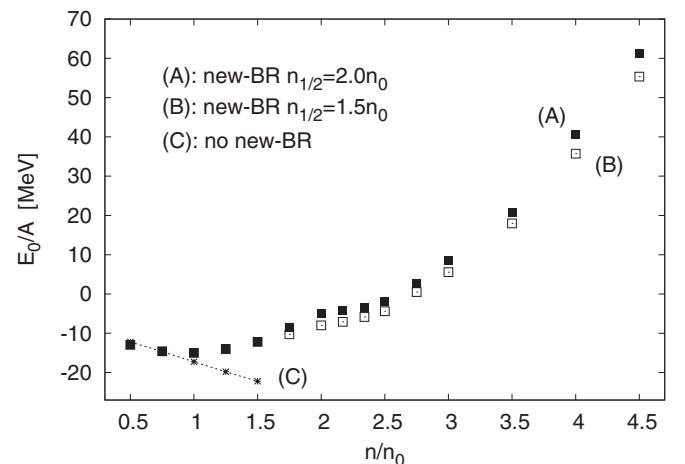

FIG. 3. Comparison of the EoS for symmetric nuclear matter calculated with $n_{1/2} = 2.0$ (solid square) and $1.5n_0$ (open square). See text for more explanations.

---

[4]Here we are doing some fine tuning for a better fit but the small differences in c_I's are of course of no significant meaning.

saturation properties ($E_0/A = -15$ MeV, $n_{sat} = 0.93n_0$, and $K = 208$ MeV).

Turning to the EoS in Region II ($n > n_{1/2}$), we note from (2.10) and (2.11) [or (3.1–3.5)] that the scalings for R_ρ^* controlling the ρ tensor force in Region II are significantly different from those in Region I: Other components of vector-meson-exchange nuclear forces are governed, apart from the mass scaling, by the scaling of the hidden gauge coupling constant,

$$g_\rho^*/g_\rho \approx g_\omega^*/g_\omega \approx 1; \quad n < n_{1/2}, \qquad (4.4)$$

$$g_\rho^*/g_\rho \approx \left[\Phi_{II}^M\right]; \quad n > n_{1/2}. \qquad (4.5)$$

Were the flavor $U(2)$ symmetry operative in Region II, the scaling (4.5) would hold for both ρ and ω. It turns out, however, that if the ω-nucleon coupling dropped in the same way as the ρ-nucleon coupling, nuclear systems would collapse in that region. We have found that the repulsion provided by the ω-exchange potential is sensitively dependent on the ω-nucleon coupling constant, and a moderate dropping of this constant can drastically suppress the repulsion, making the system unstable at high densities unless the nucleon mass dropped appreciably, which we do not consider realistic. This signals that the coupling constant g^* must be asymmetric in high density or higher members of the ω mesons in the infinite tower in holographic QCD models that arise in string theory [34] could intervene in providing the necessary repulsion. In our calculation, we will take $g_\omega^*/g_\omega \approx 1$ for both Regions I and II.

Another difference is that the scaling of the nucleon mass (m_N^*/m_N) is density dependent in Region I as is seen in experiments while it is equal to a constant or slowly varying in Region II. These differences can make the EoSs in these two regions significantly discontinuous at $n = n_{1/2}$. As mentioned above, this discontinuity could be an artifact of our schematic treatment of the skyrmion-half-skyrmion transition. We have found that this discontinuity can be made small by suitably choosing the scaling parameters in Region II. We have done so, and for the EoSs (A) and (B) presented in Fig. 3 we have used $c_{II} = c_I$ for both (A) and (B), with $y(n) = 0.77$ and $n_{1/2} = 2.0n_0$ for (A), and $y(n) = 0.78$ and $n_{1/2} = 1.5n_0$ for (B). The use of the above $y(n)$ values is to have the $n < n_{1/2}$ energy curves join smoothly with, respectively, their $n > n_{1/2}$ counterparts at $n_{1/2}$. It may be noted that both $y(n)$ values are close to 0.80. These parameter choices will be referred to, respectively, as A parameters and B parameters. They will be used and tested in other calculations such as nuclear symmetry energies and neutron stars later on. That the behaviors of m_N^* and g_ω^* may be strongly correlated in Region II will be discussed in the discussion section. In view of the almost complete absence of model-independent theoretical tools for these quantities in Region II, our strategy will then be that the available heavy-ion experiments that probe densities up to ~$4.5n_0$ give constraints on those parameters. Calculating those parameters from the given theoretical framework remains to be done.

It may be useful now to have a summary of the new-BR scalings employed in our present calculations. For this purpose, we present a plot of our m^*/m and g^*/g scalings, for the case of $n_{1/2} = 2n_0$, in Fig. 4. As shown by line (A) there,
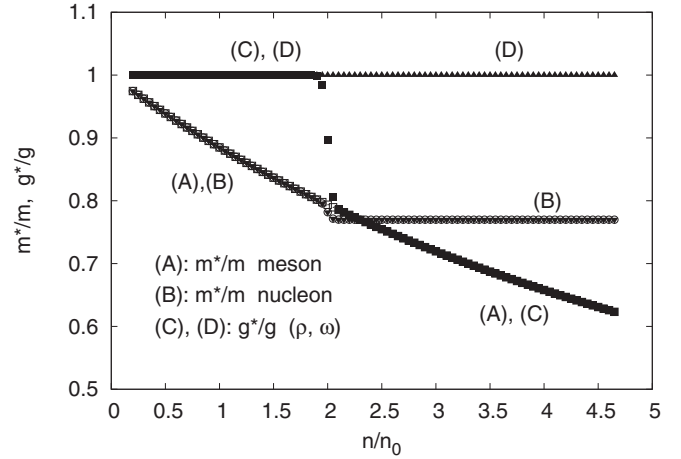

FIG. 4. Plot of new-BR scalings for Regions I and II. See text for more explanations.

the scalings for the ρ, ω, and σ masses are the same in both regions, recalling that for them we have $c_I = c_{II}$ and they are all close to 0.13. (This value is used for plotting them in the figure.) As shown by line (B), the scaling of the nucleon mass in Region I is the same as the above mesons, but in Region II it is equal to a constant $y(n)$. [$y(n) = 0.77$ is used in the figure.] From (C) and (D), we see that the scaling g^*/g for ρ is equal to one (i.e., unscaled) in Region I and equal to the above meson scaling in Region II, while the scaling for ω is equal to one in both regions.

As stated above, the above summary represents scalings of the intrinsic parameters of the underlying Lagrangian with appropriate symmetries (here, hidden local symmetry that captures the physics of vector mesons) with which our nuclear EFT is constructed. In physical quantities, the sharpness in changeover would be smoothed by many-body correlations as we find in the results.

It is of interest that the EoSs (A) and (B) of Fig. 3 both exhibit a narrow "plateaulike" segment near $n \sim 2.2n_0$. The occurrence of this plateaulike structure may indicate a skyrmion-half-skyrmion transformation which is of interest for further study.[5] This occurrence could be largely due to the use of a constant (nonscaling) nucleon mass beyond $n_{1/2}$—which we assume here—as is indicated in the half-skyrmion matter and predicted in the parity-doublet model with a large chiral-invariant mass m_0. It may be pointed out that $y(n)$ plays

---

[5]Such a changeover is generically observed on crystal: In fact a recent skyrmion crystal calculation with hidden local symmetry Lagrangian—without unknown parameters—confirmed the topological change at low enough density [35]. There is also an independent support coming from renormalization-group analysis at one-loop order for the changeover of the parameters exploited in this paper [36]. That a topological phenomenon is involved suggests that it is likely robust. The quark condensate $\langle\bar{q}q\rangle$ vanishes on average in unit cell in the crystal description but this is not a *bona fide* order parameter because the pion is present in the system, indicating chiral symmetry is not restored in the half-skyrmion state. We defer details to a later publication.

an important role in determining the EoS of nuclear matter in Region II as illustrated in Fig. 3.

For density $n > 2.0n_0$, the parameters used for the EoSs (A) and (B) there differ only in $y(n) = 0.77$ for (A) and $= 0.78$ for (B), the c_{II} parameters used for them being identical. It is seen from Fig. 3 that this small difference has made the (A) EoS significantly more repulsive than (B), especially in the high density region. Our calculations have found that the use of a smaller $y(n)$ would generally give an upward lift to the $n > n_{1/2}$ EoS, resulting in a stiffer EoS.

We have performed additional calculations studying mainly how our calculations depend on the location of the transition density $n_{1/2}$. Where it is located and how to choose is a central issue in our approach. It cannot be lower than n_0 because it will be at odds with nuclear structure as we know it. If it is far greater than n_0, then it will be inaccessible by terrestrial experiments, so will be difficult to verify its existence. As suggested in skyrmion crystal calculations [2,6], we will assume that it is located slightly above n_0. Our results reported there indicate, however, that the EoSs obtained with the new-BR scaling in the range $1.5n_0 < n_{1/2} < 2.0n_0$ depend only weakly on $n_{1/2}$ picked for all ranges of density relevant for our work. We believe that the precise location of $n_{1/2}$ is not important in our calculations as long as it is not far from n_0, while it is $y(n)$ which plays an important role.

By way of heavy-ion collision experiments, there was much progress in determining the nuclear symmetry energy E_{sym} up to densities as high as $\sim 5n_0$ [37–39]. Thus an application of our new-BR scaling to the calculation of E_{sym} would provide an important test for this scaling in the region with $n > n_{1/2}$.

The nuclear symmetry energy is related to the asymmetric nuclear matter EoS as Eq. (2.1). We have calculated $E(n, \alpha)$ for a range of α values, and from them we extract E_{sym}. Also we use the same ring-diagram formalism where the $pphh$ ring diagrams are summed to all orders. In Fig. 5 we present our results calculated with the same new-BR A and B parameters mentioned earlier, labeled, respectively, by solid and open squares there. It is of interest that the symmetry energies given

by the A and B parameters are nearly identical, despite the considerable differences between the two corresponding EoSs for symmetric nuclear matter shown in Fig. 3.

Based on heavy-ion scattering experiments, Li *et al.* [37] have suggested an empirical relation,

$$E_{\text{sym}}(n) \approx 31.6(n/n_0)^{\gamma}; \quad \gamma = 0.69 - 1.1, \quad (4.6)$$

for constraining the density dependence of the symmetry energy. The upper ($\gamma = 1.1$) and lower ($\gamma = 0.69$) constraints are also plotted in the figure, labeled, respectively, as "expt-Li1" and "expt-Li2." Also based on such experiments, Tsang *et al.* [39] recently proposed a new empirical formula for the symmetry energy, namely,

$$E_{\text{sym}}(n) = \frac{C_{s,k}}{2}\left(\frac{n}{n_0}\right)^{2/3} + \frac{C_{s,p}}{2}\left(\frac{n}{n_0}\right)^{\gamma_i}, \quad (4.7)$$

where $C_{s,k} = 25$ MeV, $C_{s,p} = 35.2$ MeV, and $\gamma_i \approx 0.7$. This formula is also plotted in Fig. 3, labeled as "expt-Tsang." Note that Tsang's results are very close to the lower constraint of Li *et al.*

Returning to Fig. 5, we see that our new-BR results agree reasonably well with the empirical constraints on E_{sym}; for Region I our results are slightly below the empirical lower bounds while in Region II they tend to be closer to the upper bound. This accounts for the EoS becoming stiffer over empirical fits as shown in Fig. 6 for neutron matter, where symmetry energy is active in its full strength with $\alpha = 1$, while the EoS for symmetric matter (with no contribution from the symmetry energy, $\alpha = 0$), lies within the empirical range as seen in Fig. 6.

Recently Lattimer and Lim [40] have investigated the constraints on E_{sym} and L [defined as $3u\,(d\,E_{\text{sym}}/du), u \equiv n/n_0$] at density $n = n_0$. The results deduced from nuclear masses, nuclear giant dipole resonances, astrophysics, neutron skins of the Sn isotopes, and other investigations exhibit wide variations, with $E_{\text{sym}}/\text{MeV}$ ranging from ~ 24 to ~ 36 and L/MeV from ~ -20 to ~ 100. The overlap constraints allowed by all these results are $29.0 \lesssim \frac{E_{\text{sym}}}{MeV} \lesssim 32.7$ and $40.5 \lesssim \frac{L}{MeV} \lesssim 61.9$ [40]. Our results as given by (A) and (B) of Fig. 4 are
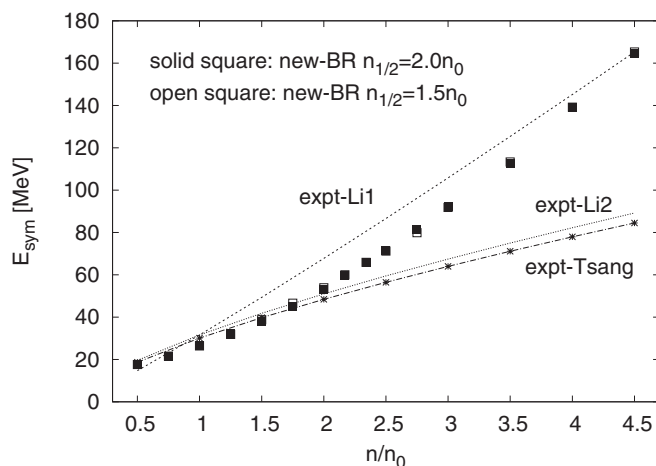

FIG. 5. Comparison of our calculated nuclear symmetry energies with the empirical upper (expt-Li1) and lower (expt-Li2) constraints of Li *et al.* [37] and the empirical results of Tsang *et al.* (expt-Tsang) [39]. See text for more explanations.
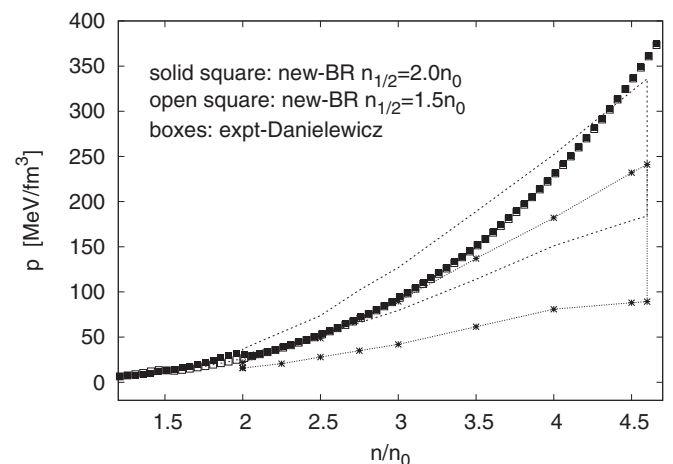

FIG. 6. Comparison of our calculated neutron matter EoS with the empirical stiff (upper box) and soft (lower box) constraints of Danielewicz *et al.* [41].

$E_{\rm sym}/{\rm MeV} \approx 26.5$ and $L/{\rm MeV} \approx 64$. $E_{\rm sym}$ is slightly lower while L is slightly higher than the above constraints, although consistent with the constraints given by the nuclear masses and nuclear giant dipole resonances. We should of course emphasize that the result that our values for $E_{\rm sym}$ and L determined near the nuclear matter density lie lower than those given by the bound, in particular for L, does not directly reflect on the quality of our new BR which brings in new ingredient in Region II following the topology change in our theory. In fact it concerns mainly the parameters of Region I which could be suitably readjusted to agree with the bound without affecting other observables. In this regard, we depart from the currently favored notion that certain dense matter theories can be ruled out by the bounds.

From heavy-ion collisions, Danielewicz *et al.* [41] have obtained constraints for the pressure-density EoS $p(n)$ of neutron matter up to densities $\sim 4.5 n_0$. To further study our new-BR scaling in the high density region, we have calculated the neutron $p(n)$ EoSs up to the above densities. A comparison of our results with their constraints is presented in Fig. 6 where the upper and lower boxes are, respectively, the constraints for the stiff and soft EoSs of [41]. Our EoSs calculated with parameters A and B are denoted by "solid-" and "open-square," respectively. A similar comparison for the $p(n)$ EoSs for symmetric nuclear matter is presented in Fig. 7. We have also calculated the speed of sound v_s in nuclear (and neutron) matter using the relation $(v_s/c)^2 = dp/d\epsilon$, ϵ and c being, respectively, the energy density and speed of light. As an illustration, our results for v_s in neutron matter are presented in Fig. 8. The results are given for the range of density for which our theory is applicable. The extrapolation procedure used to go higher in density so as to obtain the maximum star mass is described below.

As seen from Figs. 6 and 7, our calculated pressures are in satisfactory agreements with the empirical constraints of [41]. Note, however, our results are somewhat stiffer than the experimental ranges at high densities near $\sim 4 n_0$. It is instructive to look at the speed of sound v_s which is closely related to the stiffness of the EoS. It is seen from Fig. 8 that the v_s given by our new-BR scaling is significantly larger than that given by the old-BR scaling [23], indicating the former EoS being stiffer. As to be reported below, our neutron-matter EoS is,
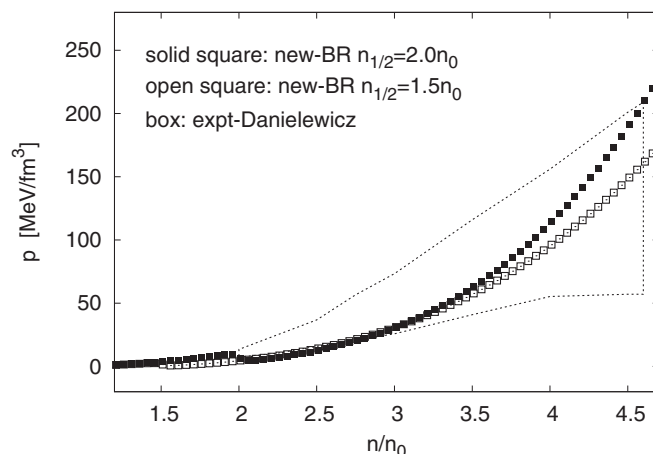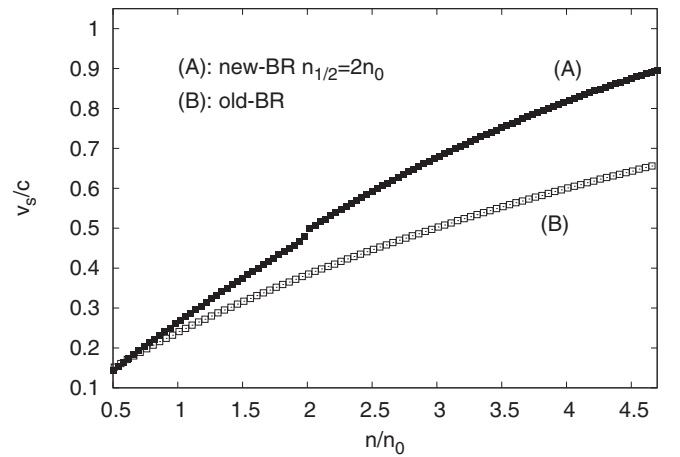
FIG. 8. Speed of sound v_s calculated with new- and old-BR scalings.

however, somewhat stiffer than what would give the two-solar mass star. There seems to be nothing obviously wrong with this. The model having the hybrid hadron-quark continuity mentioned above [42] seems to favor such massive stars.

We have not yet described how we calculate the p and v_s results shown in the above three figures. Let us do this now. Including the nucleon rest-mass energy, we first calculate the nuclear-matter energy density,

$$\epsilon(n) = n\left(\frac{E_0(n)}{A} + m_N\right), \qquad (4.8)$$

with the average ground-state energy $E_0(n)/A$ obtained from the ring-diagram method described earlier (Sec. III). The pressure-density EoS is then given by

$$p(n) = n\frac{d\epsilon(n)}{dn} - \epsilon(n). \qquad (4.9)$$

As indicated above, to calculate $p(n)$ we need to have the derivatives of the energy EoS $d\epsilon(n)/dn$ or $d(E_0(n)/A)/dn$. There is, however, a difficulty in doing so, as our $E_0(n)/A$ EoS as shown in Fig. 3 is "not" a continuous/smooth one: It is composed of two branches, one for skyrmion ($n < n_{1/2}$) and the other for half-skyrmion ($n > n_{1/2}$). These two branches have clearly different shapes (slope and curvature), and their slopes are not continuous at $n_{1/2}$. Also the EoS after $n_{1/2}$ has a short segment of plateaulike structure at $n \approx 2.2 n_0$. These features present obstacles to the calculation of the derivatives $d\epsilon(n)/dn$ and consequently hinder the calculation of $p(n)$. To circumvent this difficulty, we need to employ a fitting procedure so as to have a smooth (differentiable) $\epsilon(n)$. Such a smooth crossover is expected also in a hybrid hadron-quark matter model mentioned below [42].

Li and Schulze [43] recently proposed a highly desirable parametrization for the nuclear-matter EoS: They have found that a wide range of nuclear EoSs can be fitted very accurately by the polytrope EoS $E_0(n)/A = an + bn^c$ where a, b, and c are parameters. We have adopted this fitting procedure in our present work. With such polytrope EoSs, the pressure EoS $p(n)$ can be conveniently obtained and so is the speed of sound
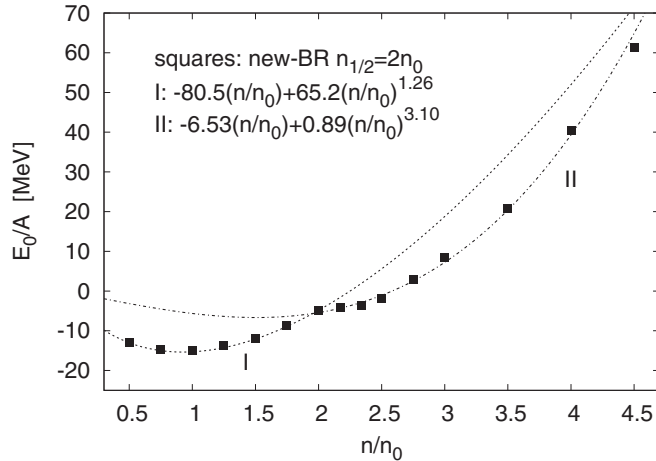
FIG. 7. Same as Fig. 5 for symmetric nuclear matter.

FIG. 9. Polytrope fits of the $n_{1/2} = 2n_0$ E_0/A EoS of Fig. 3.

v_s ($(v_s/c)^2 = dp/d\epsilon$). To illustrate this fitting, let us consider its application to the $n_{1/2} = 2n_0$ EoS of Fig. 3. We have found it impossible to fit the EoS entirely with one polytrope. But with two polytropes, one for skyrmion and another one for half-skyrmion, a satisfactory fit to the entire EoS can be achieved as shown in Fig. 9. [In our fitting, we actually use the polytrope of the form $E_0(n)/A = a(n/n_0) + b(n/n_0)^c$. In this way, the coefficients a and b have the same units (MeV) and c is dimensionless.] As seen, the fit comes out quite well. Furthermore, the a, b, and c coefficients for the two polytropes are vastly different. This is a worth-noting result, suggesting that the skyrmion and half-skyrmion EoSs are largely different "mathematically." Are they also very different physically? It should be useful and of much interest to investigate this question theoretically as well as experimentally.

Our results for the pV diagram originated from the $n_{1/2} = 2n_0$ EoS of Fig. 3 are presented in Fig. 10. Here the volume is defined as $V/V_0 \equiv n_0/n$. As seen, $p(n)$ is discontinuous at the crossover density $n_{1/2}$. Furthermore, at this point the half-skyrmion pressure is significantly lower than the skyrmion pressure. This relative difference in pressure is
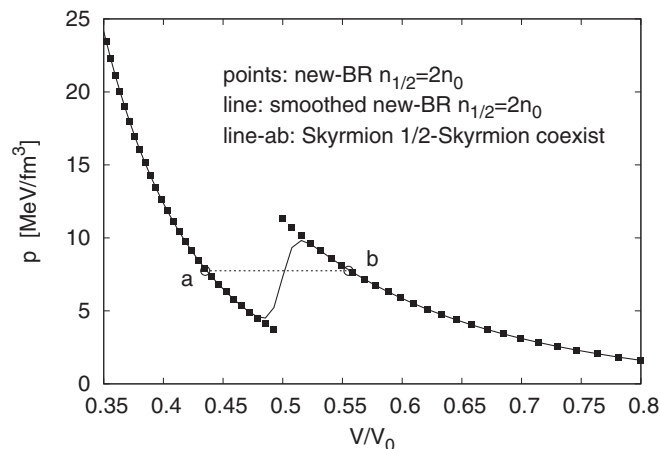

FIG. 10. Skyrmion half-skyrmion coexistence in symmetric nuclear matter calculated with $n_{1/2} = 2n_0$ new-BR scaling. The coexistence points a and b satisfy both $p(a) = p(b)$ and $\mu(a) = \mu(b)$.

a necessary condition for having a skyrmion half-skyrmion coexistence. (The coexistence would not be possible if this relative difference were reversed.) To have such a coexistence, we also need to have the two coexistence points, labeled a and b in the figure, satisfying simultaneously pressure and chemical-potential equivalences, namely $p(n_a) = p(n_b)$ and $\mu(n_a) = \mu(n_b)$. ($\mu = d\epsilon/dn$, ϵ being the energy density.) The points a and b of Fig. 8 satisfy this double requirement, with $n_a = 2.23n_0$, $n_b = 1.72n_0$, $p(n_a) = p(n_b) = 6.59$ MeV/fm^3, and $\mu_a = \mu_b = 14.61$ MeV.

The above results are for the $n_{1/2} = 2n_0$ symmetric nuclear matter using the new-BR A parameters. We have repeated this calculation for neutron matter, obtained $(n_a, n_b) = (1.93, 2.09)n_0$. The width of the coexistence region is about $0.15n_0$, considerably narrower than that for symmetric nuclear matter. For the $n_{1/2} = 1.5n_0$ calculation using the B parameters, we have obtained $(n_a, n_b) = (1.49, 1.89)n_0$ for symmetric nuclear matter, and $= (1.43, 1.59)n_0$ for neutron matter. Note that here the n_a for the symmetric nuclear matter is very close to the crossover density $n_{1/2}$ ($= 1.5n_0$). This suggests that the skyrmion half-skyrmion transition in this case is almost a pure unison crossover where the nuclear matter at $n < n_{1/2}$ is entirely composed of skyrmions, and when density increases to $n_{1/2}$ it all becomes half-skyrmion matter, leaving no buffer zone for their coexistence.

In Fig. 8, the "smoothed" pV curve is obtained by combining the two discontinuous branches using two Fermi-Dirac functions, similar to what we did in smoothly joining the scaling functions Φ_I and Φ_{II} described in Sec. III [see (3.6) and (3.7)]. The resulting pV curve is then of the standard form for coexistence, like that for the familiar liquid-gas coexistence. The above smoothing procedure has also been used for the pressure EoSs of Figs. 5 and 6.

In a recent neutron-star calculation using realistic *NN* potentials [23], the effects from the "old-BR" scaling (2.3) and (2.4) applied in both I and II were found to be highly important for neutron stars, the maximum mass, and its radius calculated (with, without) the inclusion of such effects being, respectively, ($\sim$1.8, $\sim$1.2$M_\odot$) and ($\sim$8.9, $\sim$7.2) km. Now the question is: What does the new BR (2.5) do to neutron stars? To address this question, we have calculated the properties of pure neutron stars (i.e., made of neutrons only) from the above neutron-matter EoSs, using the calculation procedures described in [23].

In Fig. 11 we present our calculated neutron-star mass-radius trajectories (A) and (B), obtained, respectively, with the A and B parameters mentioned earlier. (In this figure the symbol M_{sun} is used to denote the solar mass $M_\odot$.) The caveat mentioned above notwithstanding, it is interesting that the main results of the two calculations (A) and (B) are nearly the same. The maximum mass of neutron stars given by the two are practically identical as given in the caption of Fig. 11. It is significant that there is little dependence on the location of $n_{1/2}$ as long as it is not too high above n_0. In the low-mass region (lower right corner of the figure) the trajectories are noticeably different, with (A) having slightly larger mass and longer radius. These results are consistent with the results shown in Fig. 5 where the two EoSs are essentially equivalent to each other except in the narrow region between 1.5 and
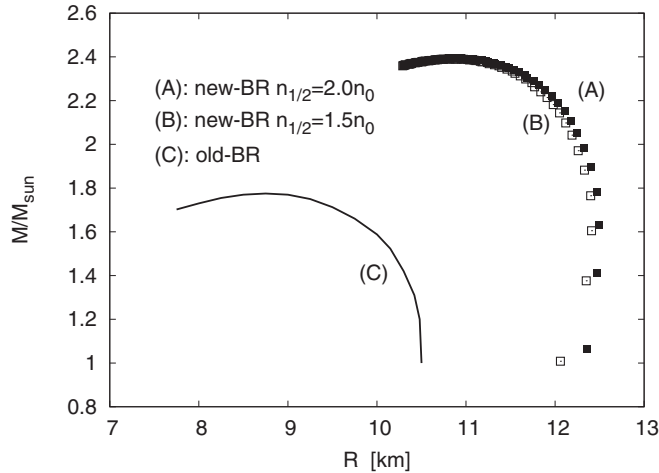
FIG. 11. Mass-radius trajectories of neutron stars calculated with new-BR scalings using $n_{1/2} = 2.0$ (A) and $1.5n_0$ (B). The maximum neutron-star mass and its radius for these two cases are, respectively, $(2.39\ M_\odot, 10.90\ \text{km})$ and $(2.38\ M_\odot, 10.89\ \text{km})$. The prediction with old-BR (C) [23] is given for comparison.

$2.0n_0$. The effects from the present new-BR scaling appear to be even stronger than those from the old-BR scaling. For example, the maximum mass obtained (with, without) the new-BR scaling are $(\sim2.4, \sim1.2M_\odot)$, the increase between them being significantly larger than the above old-BR case. As one can see in Fig. 11 (see also Fig. 12), the star properties are markedly different between the old BR and the new BR. By analyzing a wide range of empirical data, Steiner *et al.* [44] have obtained a constraint for neutron-star radius $10\ \text{km} \leqslant R \leqslant 12.5\ \text{km}$. The radius given by our new-BR calculations is in good agreement with this constraint.

In Fig. 12 we report the central densities n_{center} of the neutron stars calculated with the new-BR scalings as described above. The maximum-mass neutron stars have $n_{\text{center}} \simeq 5.5n_0$. Recalling Figs. 5 and 6, Danielewicz *et al.* [41] have provided experimental constraints for the nuclear-matter EoSs up to density $\sim4.5n_0$. This gives us important guidelines about the EoSs below this density. But beyond this, there is still no such guideline and one is really not at all sure what the EoSs there
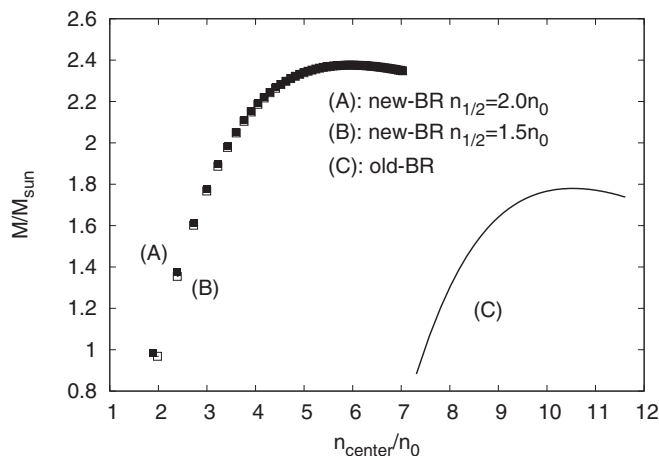

FIG. 12. Central densities (n_{center}) for the neutron stars of Fig. 9.

should be. Although we can "calculate" the EoS using our new-BR formalism up to any densities, the resulting EoS is, we believe, of "good confidence level" only for densities below and not much higher than $\sim4.5n_0$. Thus we have adopted an extrapolation scheme, namely calculating the EoS up to an extrapolation density n_{ext} while obtaining the EoS beyond this density by a polytrope extrapolation. (The polytrope is obtained by fitting the EoS below n_{ext}.) The mass of neutron star with central density of n_{ext} is $\sim2.3M_\odot$.

Clearly this extrapolation can be applied only to densities not too much higher than n_{ext}. We have employed $n_{\text{ext}} = 4.5$ and $5.5n_0$ and found that the EoSs given by them are in close agreement with each other up to $\sim7.0n_0$. This and that our n_{central} is as small as $\sim5.5n_0$ support the reliability of the above extrapolation procedure for our present neutron-star calculations. The causal limit in this extrapolation lies at $5.9n_0$, which is larger than the central density of $5.5n_0$ for the maximum mass in Figs. 11 and 12. It would be very interesting to study the EoS for neutron stars with RIB machines as the low central densities of neutron stars as given earlier should be readily accessible there. As stated earlier, our present calculation has assumed a pure neutron-matter composition for neutron stars without taking into account a variety of compact-star conditions. This could be an oversimplification, and the results obtained thereby should be taken, at best, indicative of what could be happening in nature.

V. COMMENTS AND DISCUSSIONS

In this paper, we subjected the nuclear effective field theory anchored on RG flow, with the parameters of the Lagrangian sliding with density, to normal nuclear matter and dense compact-star matter. The scaling behavior used here differs from the old BR scaling [12], in that at a density $n_{1/2} > n_0$, a topological change takes place from skyrmion matter to half-skyrmion matter, giving rise to a modified scaling new BR. The changeover from skyrmion matter to half-skyrmion matter is characterized by a vanishing quark condensate $\langle \bar{q}q \rangle = 0$ but a nonvanishing pion decay constat $f_\pi \neq 0$. Thus it is not a standard phase transition à la Ginzburg-Landau-Wilson paradigm although two different phases are involved; it appears to involve an emergent symmetry not present in the fundamental theory, QCD.

At the semiclassical approximation made in the calculation, the half-skrymions are not deconfined in contrast to what happens in certain condensed matter systems [45]. They are bound or confined, so they are not propagating degrees of freedom. What characterizes the system is that the mass of the baryon made up of two "bound" half-skyrmions remains more or less unscaled, not going to zero up to the density n_c at which the quarks get deconfined, whereas the ρ-meson mass is expected to drop faster in the half-skyrmion phase than in the skyrmion phase. This means that the origin of the most, if not all, of the nucleon mass is not in the dynamical symmetry breaking of chiral symmetry, in contrast to the meson mass, with a substantial mass of the nucleon coming from a hitherto unknown source. This is similar to what is described in the parity-doublet model of the nucleon [14,46]. We should note, however, that this picture is clearly at odds with the constituent

quark model—which has a strong theoretical support from QCD in the large N_c limit [47]—where the ratio of the meson mass over the baryon mass is 2/3. Whether or not the constituent quark model is applicable in nuclear medium is not known, but if there were an m_0 for the quark which is not small, then it should be possible that the constituent quark model hold in dense medium and the ratio remain more or less the same. In this case, the scaling could be considerably different from the new BR.

It is intriguing that the two consequences of the changeover at $n_{1/2}$, namely, the drastic modification of the nuclear tensor force and the stiffening of the EoS of dense matter at $n_{1/2}$, seem to be hinting at the mechanism for the generation of ~99% of the nucleon mass in the strong interactions. See [48] for discussions on this matter.

The salient features obtained in the RG-implemented effective theory approach adopted in this paper can be summarized as follows:

(i) Without a suitable scaling in the Lagrangian that figures in $V_{\mathrm{low}-k}$ (or incorporating many-body forces), symmetric nuclear matter cannot be stabilized at the right density and with correct binding energy.

(ii) Our calculations have essentially two scaling parameters: one is $c_I \approx 0.13$ for all mesons (vector mesons and scalar meson) and the nucleon in region I, and in region II we have $c_{II} = c_I$ for mesons and the vector coupling and an additional parameter $y(n) \approx 0.8$ for the nucleon. With these two parameters, one can explain satisfactorily the saturation density, the binding energy and the compression modulus of symmetric nuclear matter as well as the nuclear symmetry energy, and predict the EoSs for symmetric and asymmetric nuclear matter at high density and compact-star matter. Our results give a good fit to all quantities that are available experimentally at densities up to $n \sim 4n_0$.

(iii) The topology change from skyrmion to half-skyrmion at $n_{1/2}$ changes the slope of the EoS, making it stiffer in the half-skyrmion phase and raises the maximum mass of compact stars to ~$2.4M_\odot$. Verifying the presence and the role of the topology change at $n_{1/2}$ should be feasible at RIB machines.

In our treatment, n-body forces for $n > 2$ have not been taken into account. As mentioned, three-body forces—in place of BR—could equally well provide the repulsion needed to stabilize nuclear matter. This does not mean that the many-body forces and the BR are alternatives. They should both come in together. In principle, there should be no problem in including both BR and many-body forces in a way consistent with the tenet of chiral expansion. What one has to do in the presence of such n-body potentials is then to suitably modify the scaling properties of the Lagrangian, because direct and indirect chiral symmetry effects are compounded in physical quantities in a variety of different chiral expansion schemes as illustrated in [49]. A fully consistent way of doing the calculation would be to have *both* the scaling and many-body potentials treated together with certain constraints, such as thermodynamic consistency, taken into account. We also note that our EoS is very close to the EoS found in Ref. [40] with a

similar stiffening throughout the range of density considered, where the sound velocity never exceeds 0.9.

We have not taken into account strangeness degrees of freedom—such as kaons, hyperons, strange quarks, etc.—into the EoS for neutron-rich matter. In our formulation anchored on dense skyrmion matter, as described in [7], hyperons can enter only *after* kaons condense. Therefore the issue here is how kaon condensation can take place after changing from skyrmion matter to half-skyrmion matter.

There are two opposing mechanisms to consider in the process. One is that in the presence of the topology change at $n_{1/2}$, the mass of K^- has a propitious drop not present in conventional chiral perturbation treatments [50]. This goes in the direction of lowering the critical density for kaon condensation. The other is the effect of stiffening the EoS. It is known, for instance, in phenomenological studies that the more repulsion there is in nonstrange nuclear interactions, the higher the kaon condensation critical density goes up [51]. What will happen in compact stars therefore will depend crucially on which one dominates. One intriguing possibility is that the stiffening postpones the drop of m_K^* in a manner analogous to the stiffening at the smooth crossover at a density ~$(2-4)n_0$ from hadron to nonstrange quark phase in the hybrid model that also yields the maximum star mass ~$2.3M_\odot$ [42]. This will also have an important impact on the cooling of the star, because the appearance of strange flavor at higher density will prevent fast direct URCA process from setting in too precociously.

It should be stressed that in our approach, strangeness in the form of condensed kaons (or equivalently hyperons) may enter at near or even before the density to which our theory with topology change can be extended, say ~$4.5n_0$. Therefore the extrapolation beyond such density with polytropes, without accounting for strangeness degrees of freedom, potentially violating causality, should be taken as merely exploratory.

One important aspect in our treatment that requires serious studies is the correlation between the behavior of the in-medium nucleon mass m_N^* and that of the in-medium ω-N coupling $g_{\omega NN}$ which is related to the $U(1)$ gauge coupling g_ω^*. We have adopted in our calculation the information from the skyrmion crystal calculations [5,34] and the parity-doubling nucleon model [46] that the nucleon mass drops only about 20% up to the highest density we are considering. We have taken the scaling y effective in Region II to be constant as indicated in the skyrmion-crystal calculation [34] and in the one-loop RG analysis of HLS Lagrangian. As stated, were we to drop the ω-nucleon coupling according to $g_\omega^*/g_\omega \approx g_\rho^*/g_\rho \approx g^*/g = \Phi_{II}$ as one would expect if flavor $U(2)$ symmetry held in Region II, the EoS would become much too soft above n_0 to be compatible with the existence of the two-solar mass object observed in nature. We kept $g_\omega^*/g_\omega \approx 1$ while letting the ω mass scale. Now to quantify the above observation, we have examined the effect of dropping ω-NN coupling for given m_N^*s. Writing the ω-nucleon coupling in Region II as $g_\omega^*/g_\omega = (1 + c_{II,N\omega}n/n_0)^{-1}$, we have found at $n = 2.5n_0$, $E_0/A = (-33.9, -50.9, -68.4)$ MeV for $y(n) = 0.77$ and $E_0/A = (11.68, -1.26, -14.56)$ MeV for $y(n) = 0.60$ for the scaling constant of the ω-NN coupling $c_{II,N\omega} = (0.046, 0.093, 0.139)$ with all other parameters fixed to (A)

of Fig. 3. One sees that the EoS is extremely sensitive to the in-medium properties of both the nucleon mass and the ω-NN coupling.

There are two implications that follow from this calculation. One is that $U(2)$ symmetry can be badly broken in dense medium and as a consequence the vector manifestation of HLS [10] does not apply to the in-medium ω meson although its mass may approach zero as the ρ mass does à la mended symmetry. The other is that the in-medium nucleon mass and ω-NN coupling must be strongly correlated. One-loop renormalization group equations with the generalized hidden local symmetry Lagrangian implemented with baryons (with no dilatons) of [46] show that in the chiral limit, both m_ρ^* and m_ω^* approach zero as the dilaton limit fixed point is approached. So does the nucleon mass m_N^* in the standard (or "naive") assignment for the nucleon (see [46]). However, while the vector manifestation of HLS [10] requires that $g_\rho^*/g_\rho \propto \langle\bar{q}q\rangle^*/\langle\bar{q}q\rangle \to 0$ near chiral restoration, if $U(2)$ symmetry is violated in medium, the in-medium ω-NN is predicted to drop much more slowly than the ρ-NN coupling [46]. At one-loop

order the ω-nucleon coupling is found not to scale. It is only at two-loop and higher order that scaling sets in. One can see from the RGEs the interplay between the slow scalings of the coupling and nucleon mass. This behavior agrees qualitatively with what was noticed above where lowering the nucleon mass required reducing the coupling g_ω to have the symmetry energy lie within the range given by heavy-ion data.

[1] T. H. R. Skyrme, Nucl. Phys. **31**, 556 (1962).

[2] G. E. Brown and M. Rho (eds.), *The Multifaceted Skyrmion* (World Scientific, Singapore, 2010).

[3] S. Heinze *et al.*, Nat. Phys. **7**, 713 (2011).

[4] A. S. Golhaber and N. S. Manton, Phys. Lett. B **198**, 231 (1987).

[5] B. Y. Park, D. P. Min, M. Rho, and V. Vento, Nucl. Phys. A **707**, 381 (2002); H. J. Lee *et al.*, *ibid.* **723**, 427 (2003); M. Rho, arXiv:0711.3895.

[6] H. K. Lee, B. Y. Park, and M. Rho, Phys. Rev. C **83**, 025206 (2011).

[7] H. K. Lee and M. Rho, arXiv:1201.6486.

[8] H. Dong, T. T. S. Kuo, and R. Machleidt, Phys. Rev. C **83**, 054002 (2011).

[9] P. B. Demorest *et al.*, Nature (London) **467**, 1081 (2010).

[10] M. Harada and K. Yamawaki, Phys. Rep. **381**, 1 (2003).

[11] H. K. Lee and M. Rho, Nucl. Phys. A **829**, 76 (2009).

[12] G. E. Brown and M. Rho, Phys. Rev. Lett. **66**, 2720 (1991).

[13] G. E. Brown and M. Rho, Phys. Rep. **396**, 1 (2004).

[14] C. E. DeTar and T. Kunihiro, Phys. Rev. D **39**, 2805 (1989).

[15] G. E. Brown and M. Rho, Phys. Lett. B **237**, 3 (1990).

[16] J. W. Holt, G. E. Brown, T. T. S. Kuo, J. D. Holt, and R. Machleidt, Phys. Rev. Lett. **100**, 062501 (2008).

[17] G. E. Brown and R. Machleidt, Phys. Rev. C **50**, 1731 (1994).

[18] A. Li and B.-A. Li, arXiv:1107.0496; I. Vadanã, A. Polls and C. Providência, arXiv:1107.5412; F. Sammarruca, Phys. Rev. C **84**, 044307 (2011).

[19] J. W. Holt, N. Kaiser, and W. Weise, Phys. Rev. C **79**, 054331 (2009); P. Maris, J. P. Vary, P. Navratil, W. E. Ormand, H. Nam, and D. J. Dean, Phys. Rev. Lett. **106**, 202502 (2011).

[20] R. Machleidt, in *Computational Nuclear Physics 2–Nuclear Reactions*, edited by K. Langanke, J. A. Maruhn, and S. E. Koonin (Springer, New York, 1993), Chap. 1, p. 1.

[21] R. Machleidt, Adv. Nucl. Phys. **19**, 189–376 (1989).

[22] L. W. Siu, J. W. Holt, T. T. S. Kuo, and G. E. Brown, Phys. Rev. **79**, 0540004 (2009).

[23] H. Dong, T. T. S. Kuo, and R. Machleidt, Phys. Rev. C **80**, 065803 (2009).

[24] L. W. Siu, T. T. S. Kuo, and R. Machleidt, Phys. Rev. C **77**, 034001 (2008).

[25] H. Dong, L. W. Siu, T. T. S. Kuo, and R. Machleidt, Phys. Rev. C **81**, 034003 (2010).

[26] S. K. Bogner, T. T. S. Kuo, L. Coraggio, and A. Covello, Nucl. Phys. A **684**, 432 (2001).

[27] S. K. Bogner, T. T. S. Kuo, L. Coraggio, A. Covello, and N. Itaco, Phys. Rev. C **65**, 051301(R) (2002).

[28] S. K. Bogner, T. T. S. Kuo, and A. Schwenk, Phys. Rep. **386**, 1 (2003).

[29] S. K. Bogner, T. T. S. Kuo, A. Schwenk, D. R. Entem, and R. Machleidt, Phys. Lett. B **576**, 265 (2003).

[30] R. Rapp, R. Machleidt, J. W. Durso, and G. E. Brown, Phys. Rev. Lett. **82**, 1827 (1999).

[31] T. Hatsuda and S. H. Lee, Phys. Rev. C **46**, R34 (1992).

[32] M. Ericson, Phys. Lett. B **301**, 11 (1993).

[33] J. Gasser, H. Leutwyler, and M. E. Sainio, Phys. Lett. B **253**, 252 (1991).

[34] See, e.g., T. Sakai and S. Sugimoto, Prog. Theor. Phys. **113**, 843 (2005).

[35] Y.-L. Ma, M. Harada, H. K. Lee, B.-Y. Park, Y. Oh, and M. Rho (in preparation).

[36] W.-G. Paeng, H. K. Lee, M. Rho, and C. Sasaki, arXiv:1303.2898.

[37] B. A. Li and L. W. Chen, Phys. Rev. C **72**, 064611 (2005).

[38] B. A. Li, L. W. Chen, and C. M. Ko, Phys. Rep. **464**, 113 (2008).

[39] M. B. Tsang, Y. Zhang, P. Danielewicz, M. Famiano, Z. Li, W. G. Lynch, and A. W. Steiner, Phys. Rev. Lett. **102**, 122701 (2009).

[40] J. M. Lattimer and Y. Lim, arXiv:1203.4286; K. Hebeler, J. M. Lattimer, C. J. Pathick, and A. Schwenk, arXiv:1303.4662.

[41] P. Danielewicz, R. Lacey, and W. G. Lynch, Science **298**, 1592 (2002).

[42] K. Masuda, T. Hatsuda, and T. Takatsuka, Astrophys. J. **764**, 12 (2013); arXiv:1212.6803.

[43] Z. H. Li and H. J. Schulze, Phys. Rev. C **78**, 028801 (2008).

[44] B. W. Steiner, J. M. Lattimer, and E. F. Brown, Astroph. J. **722**, 33 (2010).

[45] T. Senthil *et al*., Science **303**, 1490 (2004).

[46] W.-G. Paeng, H. K. Lee, M. Rho, and C. Sasaki, Phys. Rev. D **85**, 054022 (2012); C. Sasaki, H. K. Lee, W.-G. Paeng, and M. Rho, *ibid.* **84**, 034011 (2011).

[47] S. Weinberg, Phys. Rev. Lett. **105**, 261601 (2010).

[48] M. Rho, arXiv:1301.0066.

[49] B. Friman and M. Rho, Nucl. Phys. A **606**, 303 (1996).

[50] B. Y. Park, J. I. Kim, and M. Rho, Phys. Rev. C **81**, 035203 (2010).

[51] V. R. Pandharipande, C. J. Pethick, and V. Thorsson, Phys. Rev. Lett. **75**, 4567 (1995).